Fractional Quantum Hall Physics in Jaynes-Cummings-Hubbard Lattices

Andrew L. C. Hayward,[1] Andrew M. Martin,[1] and Andrew D. Greentree[1,2]
[1]*School of Physics, University of Melbourne, Victoria 3050, Australia*
[2]*Applied Physics, School of Applied Sciences, RMIT University, Victoria 3001, Australia*
(Received 8 December 2011; published 1 June 2012)

Jaynes-Cummings-Hubbard arrays provide unique opportunities for quantum emulation as they exhibit convenient state preparation and measurement, as well as *in situ* tuning of parameters. We show how to realize strongly correlated states of light in Jaynes-Cummings-Hubbard arrays under the introduction of an effective magnetic field. The effective field is realized by dynamic tuning of the cavity resonances. We demonstrate the existence of Laughlin-like fractional quantum Hall states by computing topological invariants, phase transitions between topologically distinct states, and Laughlin wave function overlap.

DOI: 10.1103/PhysRevLett.108.223602 PACS numbers: 42.50.Pq, 32.80.Qk, 73.43.−f

Quantum systems with highly correlated states exhibit an exponential growth of Hilbert space with the number of particles, making the study of arbitrary states of even modest systems computationally intractable. This problem has motivated efforts in the field of quantum emulation [1]. A quantum emulator is designed to replicate the physics of some target system. Such emulators require scalable and convenient state preparation and measurement, and control over single- and many-body interactions. Proposals for emulation platforms include ultracold atoms, superconductors, and superfluids [2–4]. Another interesting platform is coupled atom-cavity systems [5–9] and there has been significant progress toward realizing this goal [10–13]. Here, we explore the physics of the fractional quantum Hall effect (FQHE) as it relates to atom-cavity systems.

Thirty years after their discovery, the integer [14] and fractional [15] quantum Hall effects are still the focus of intense theoretical and experimental attention [16,17]. The FQHE relies on the presence of particle-particle interactions to form highly correlated states. These states can exhibit anyonic, and sometimes non-Abelian, excitations that are explicitly nonlocal. As such, the investigation of large systems suffers strongly from the exponential explosion in Hilbert space. While there exist exact solutions for some FQHE systems, such as the Laughlin ansatz [18], these have yet to be observed directly in experiment. For this reason, emulation of the FQHE, particularly emulating the strong magnetic fields required, has become a major topic of interest in the scientific community [19–22].

Here, we show the existence of Laughlin-like FQHE states in the Jaynes-Cummings-Hubbard (JCH) model [5–7] in the presence of an artificial magnetic field. These states constitute new, strongly correlated states of light. A JCH lattice consists of an array of coupled photonic cavities, with each cavity mode coupled to a two-level atom [Figs. 1(a) and 1(b)]. JCH systems promise unparalleled control and readout of the full quantum mechanical wave function. The JCH model is predicted to exhibit a number of solid state phenomena, including Mott or superfluid phases [6], semiconductor physics [23], Josephson effect [24], metamaterial properties [25], and Bose-glass phases [26].

We begin by introducing the JCH model, and discuss how an artificial magnetic field can be created in a photonic cavity system. To demonstrate FQHE physics, we compute the ground states for small systems. These ground states are compared to a modified Laughlin ansatz, and their topology is investigated.

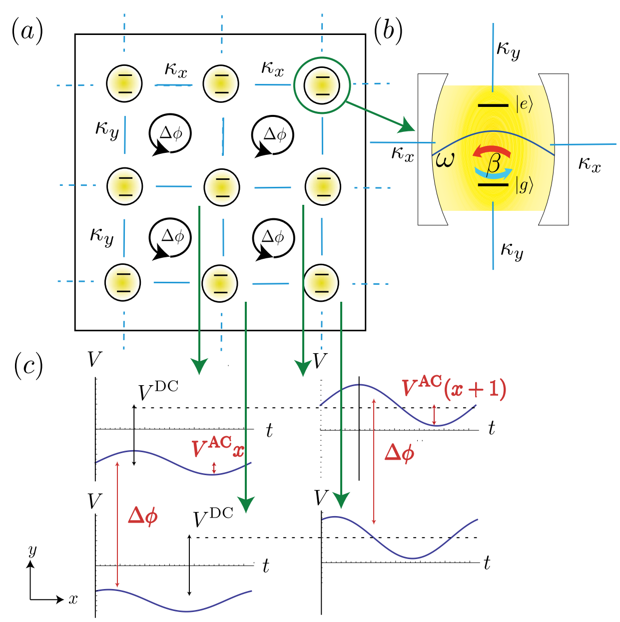

FIG. 1 (color online). (a) Schematic of a square JCH lattice with a constant effective magnetic field. Photons moving around a plaquette acquire a phase $\Delta\phi$. (b) A single-mode photonic cavity with frequency ω coupled to a two-level atom with strength β. (c) Scheme for breaking TRS in photonic cavities: a potential $V = [V^{\mathrm{DC}} + V^{\mathrm{AC}} \sin(\omega^{\mathrm{rf}} t + \Delta\phi y)]x$ (x and y in units of the lattice spacing) is applied to the cavities (indicated by thick vertical green arrows) by dynamically tuning ω. The phase offset, $\Delta\phi$, along y results in the synthetic magnetic field seen in (a).

Each cavity in the JCH lattice is described by the Jaynes-Cummings (JC) Hamiltonian

$$H^{\mathrm{JC}} = \omega L + \Delta\sigma^{+}\sigma^{-} + \beta(\sigma^{+}a + \sigma^{-}a^{\dagger}), \qquad (1)$$

where a is the photonic annihilation operator, $\sigma^{\pm}$ are the atomic raising and lowering operators, Δ the atom-photon detuning, β the coupling energy, and $\hbar = 1$. The state $|g(e), n\rangle$, where n is the number of photons, and $g(e)$ are the ground (excited) state of the atom, form the single cavity basis. H^{JC} commutes with the total excitation number operator, $L = a^{\dagger}a + \sigma^{+}\sigma^{-}$. Therefore, the total excitations in the cavity, ℓ, is a good quantum number. The eigenstates of Eq. (1) are termed polaritons, superpositions of atomic and photonic excitations, and are a function of ℓ and Δ/β.

The JCH model describes a tight-binding JC lattice:

$$H^{\mathrm{JCH}} = H^{\mathrm{JC}} + K = \sum_{i}^{N} H_i^{\mathrm{JC}} - \sum_{\langle i,j\rangle} \kappa_{ij} a_i^{\dagger} a_j, \qquad (2)$$

where κ_{ij} is the tunneling rate between cavities i and j and the sum over $\langle i, j\rangle$ is between nearest neighbors only.

For large detuning ($|\Delta| \gg \beta$), eigenstates separate out into either atomic or photonic modes. In this limit, the photonic or atomic mode can be adiabatically eliminated. Eliminating the atomic modes, the photonic mode has a weak Kerr-type photon-photon repulsion [8] and the exchange of energy between atomic and photonic modes is strongly suppressed. However, virtual processes lead to effective interactions in the photonic and atomic submanifolds. Photons have an atomic mediated nonlinear on-site repulsion, making the JCH model equivalent to the Bose-Hubbard (BH) model [27]. Atomic modes are coupled with the effective hopping rate $\kappa_{ij}^{\mathrm{eff}} = \kappa_{ij}\beta^2/\Delta^2$ [28]. As the atomic modes are restricted to two levels, this is effectively a hard-core boson field for atomic states, in contrast to the weakly interacting photon field.

The QHE occurs in a 2DEG in the presence of a perpendicular magnetic field, which breaks time reversal symmetry (TRS). Any mechanism that breaks TRS manifests in the Hamiltonian as a vector potential. An artificial magnetic field may then be realized via the introduction of some TRS breaking interaction. Constant rotation or linear acceleration are the classic examples, leading to constant synthetic magnetic and electric fields, respectively. Cho *et al.* [29] propose a scheme for TRS breaking in multimode cavities with far detuned atoms. Fang *et al.* [30] use magneto-optical resonators in photonic crystals to break TRS, and Koch *et al.* [31,32] have recently shown TRS breaking in the context of circuit quantum electrodynamics (QED), via the introduction of a special passive coupling element between microwave resonator junctions. Here, we adapt the methodology proposed by Kolovsky [21] to cavity QED, where photon-assisted tunneling is used to break TRS. An electric field with both dc and ac components is applied across one of the lattice axes [Fig 1(c)]. Introducing a phase offset, $\Delta\phi$, in the ac field along the other axis results in the desired complex coupling, $2\pi\alpha = \Delta\phi$. The presence of the two fields also leads to modified strengths of κ, Δ, and β, which can be tuned appropriately to recover the Hamiltonian in Eq. (1). The dependence of these parameters on the field is nontrivial, but follows the prescription in [21]. Photons do not respond to electric fields; however, a gradient in the cavity frequency has an equivalent effect. Recently, cavities with tunable resonances have been fabricated [33,34]. This process is achieved by the inclusion of an intracavity Josephson junction, which changes the cavity boundary conditions, and can be tuned via a magnetic field. Transmission-line resonator experiments [33] have shown ω^{rf} can be driven at $\mathcal{O}(10^3)$ times the cavity dissipation frequency. This ratio provides sufficient time to observe FQH physics.

A magnetic field is defined by a vector potential $\mathbf{A}(x)$ and is introduced into the Hamiltonian via the minimal substitution, $\mathbf{p} \rightarrow \mathbf{p} - q\mathbf{A}(x)$. On a tight-binding lattice, a vector potential $\mathbf{A}$ gives rise to a complex hopping rate $\kappa_{ij} \rightarrow \kappa_{ij}e^{i2\pi\theta_{ij}}$, where $2\pi\theta_{ij} = \int_{r_i}^{r_j}\mathbf{A}(r)dr$. As in the continuum case, gauge symmetry implies that the only physically important parameter is the total phase, $2\pi\alpha$, picked up around a closed loop, where $\alpha = \Phi/\Phi_0$ is the fraction of flux quanta through the loop. A constant magnetic field in the z direction corresponds to a constant α for all plaquettes on the lattice. Factors of 2π in the phase around a loop are physically inconsequential, so we only need consider $\alpha \in (0, 1)$. In a lattice, the effect of larger magnetic field strengths saturates, as distinct from the continuum case, where the cyclotron frequency, proportional to the magnetic field, has no upper bound.

Ignoring the JC term in Eq. (1), the spectrum for the kinetic term, K, is given by solutions to Harper's equation, resulting in the famous Hofstadter butterfly [35], a fractal structure that has q bands at $\alpha = p/q$, $(p, q) \in \mathbb{Z}$. For a single excitation on the JCH lattice, the Shrödinger equation is

$$\sum_i E\psi_i = \sum_i^N [H^{\mathrm{JC}}\psi_i - \kappa K_{ij}(\alpha)\psi_j]. \qquad (3)$$

Substituting an eigenvector ψ_i^K of K with energy k_i into Eq. (3) yields a single-site Hamiltonian:

$$H^{\mathrm{JC}}(k) = H_0^{\mathrm{JC}} + k_i\kappa a^{\dagger}a,$$

which is transformed to H_0^{JC} by $\Delta \rightarrow \Delta + k_i$. Thus, the energies and eigenstates are

$$E_{i,\pm} = -(\Delta + E_i^H)/2 \pm \sqrt{\beta^2 + (\Delta - E_i^H)^2/4},$$
$$\psi_{i,\pm} = \psi_i^K \otimes \psi_{\pm}^{\mathrm{JC}}(\Delta - k_i\kappa).$$

When the detuning is small ($\Delta \approx 0$), there are two squashed Hofstadter butterflies with a gap [Fig. 2(a)].

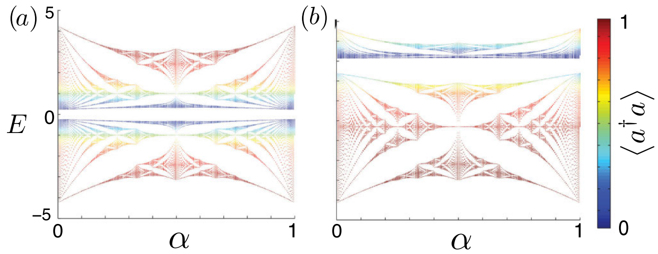

FIG. 2 (color online). Single particle spectrum of the JCH lattice with (a) $\Delta = 0$ and (b) $\Delta = 3$. In each case $\kappa = 1$ and $\beta = 1$. The spectra comprise two transformed Hofstadter butterflies. Color indicates the projection into the photonic modes.

As the relative JC interaction strength β decreases, the two parts converge to recover the original butterfly.

As previously discussed, a large detuning separates out the atomic and photonic states, as shown in Fig. 2. The spectrum is a butterfly with width $\pm 4\kappa$ centered around $-\beta^2/\Delta$, corresponding to the photonic part, and one with width $\pm 4\kappa^2/\Delta$ centered around $\Delta + \beta^2/\Delta$ [Fig. 2(b)].

The FQHE occurs for systems at sufficiently low temperatures where the flux filling factor $\nu = N_p/N_\phi$ is some nonintegral rational $\nu = p/q$, with N_p particles and N_ϕ total flux quanta. Here, particles lie predominantly in the lowest Landau level (LLL). When there is an interparticle interaction, the ground state has long-range off-diagonal order and an energy gap.

We study the FQHE on a JCH lattice with periodic boundary conditions to avoid edge effects and focus on the $\nu = 1/2$ state, which is the most stable and accessible fraction for bosons, compared to the $\nu = 1/3$ found in the electronic case. Choosing a lattice of dimensions L_x and L_y and the number of excitations N_p fixes $\alpha = 2N_p/L_xL_y$. As the state space grows quickly, we are constrained to the small systems in Table I.

The simplest FQHE states are described by the Laughlin ansatz, which is an exact solution for particles in a magnetic field with a contact interaction, and $\nu = 1/q$. Thus, for a lattice where the interparticle interaction is only on site, such wave functions can be very good approximations to the true ground state. The excitations of these states have Abelian anyonic statistics.

TABLE I. Results for systems of size $L_x \times L_y$ sites with N_p excitations. All systems have $C_1 = 1/2$ below the transition strength $\Delta = \Delta_c$. Also shown are the Hilbert space dimensions [36] Dim(H) and the Laughlin overlap.

	$L_x \times L_y$	N_p	Dim(H)	α	Laughlin overlap	Transition(Δ_c)
i	4×4	2	512	0.25	0.89	
ii	5×5	2	1250	0.16	0.99	−1.1
iii	6×6	2	2592	0.11	0.99	2.5
iv	4×4	3	5472	0.37	0.29	−9.1
v	5×5	3	20 850	0.24	0.98	−3.8
vi	6×6	3	62 232	0.17	0.99	

The Laughlin wave function with periodic boundary conditions is

$$\Psi_L(\bar{z}) \propto F_{\rm cm}(Z) f_{\rm rel}(\bar{z}) \prod_i \psi_i^L, \tag{4}$$

where $F_{\rm cm}(Z)$ is a function of the center of mass $Z = \sum_i^{N_p} z_i$, and $f_{\rm rel}(\bar{z})$ depends only on the relative particle separations:

$$F_{\rm cm}(Z) = \theta\begin{bmatrix} N_p/q + (N_\phi - 2)/2q \\ -(N_\phi - 2)/q \end{bmatrix}\left(q\frac{Z}{L_x}\,\middle|\, iq\frac{L_y}{L_x}\right),$$

$$f_{\rm rel}(\bar{z}) = \prod_{i<j}^{N_p} \theta_1\left(\frac{z_i - z_j}{L_x}\,\middle|\, i\frac{L_y}{L_x}\right)^q, \tag{5}$$

where θ is the generalized Jacobi theta function [37], and θ_1 the odd theta function. ψ_i^L are the single-particle states $e^{-y_i^2/4}$ of the LLL.

For bosons (fermions) q must be even (odd) so that Ψ has the appropriate symmetry. We define a version of the Laughlin wave function for states on a JCH lattice by replacing the single-particle Landau wave functions ψ^L with a corresponding single-polariton JCH wave function. This approximation allows the computation of the overlap between the explicit ground state of $H^{\rm JCH}(\alpha)$ and the Laughlin ansatz. Direct product states of single JCH states are not defined at points with multiple excitations; however, as $\Psi(\bar{z}) = 0$ for any $z_i = z_j$, the issue is avoided.

Significant overlap between our numerical results and the Laughlin ansatz can be a good indication of the FQHE. In Fig. 3(b), the overlap is shown as a function of Δ for each configuration. In the hard-core boson limit ($\Delta \gg 0$), our results match those found in Ref. [38]. As the on-site interaction is reduced, multiple site occupancy can occur, and overlaps with the trial wave function decrease. To fully quantify the ground state, two additional quantities need to be computed: (i) the topology of the state and (ii) the energy gap. The Chern number quantifies the topology and provides an unambiguous indication of FQHE physics [39]:

$$C_1 = \frac{1}{2\pi}\int d\theta_x\theta_y \left\langle\frac{\partial\Psi}{\partial\theta_x}\,\middle|\,\frac{\partial\Psi}{\partial\theta_y}\right\rangle - \left\langle\frac{\partial\Psi}{\partial\theta_y}\,\middle|\,\frac{\partial\Psi}{\partial\theta_x}\right\rangle, \tag{6}$$

where $\theta_{x,y}$ are the generalized periodic boundary conditions on the lattice:

$$t_x^i(L_x)\Psi = \Psi e^{i\theta_x} \qquad t_y^i(L_y)\Psi = \Psi e^{i\theta_y} \tag{7}$$

with $t_{x,y}^i$ the x and y magnetic translation operators on particle i. Varying $\theta_{x,y}$ induces an electric field on the surface of the lattice, leading to the relationship between the Hall conductance and Chern number via the Kubo formula: $\sigma_H \propto C_1$ (see Ref. [39] for a full discussion). Hence, the topology of the ground state with periodic boundary conditions is directly related to the quantization

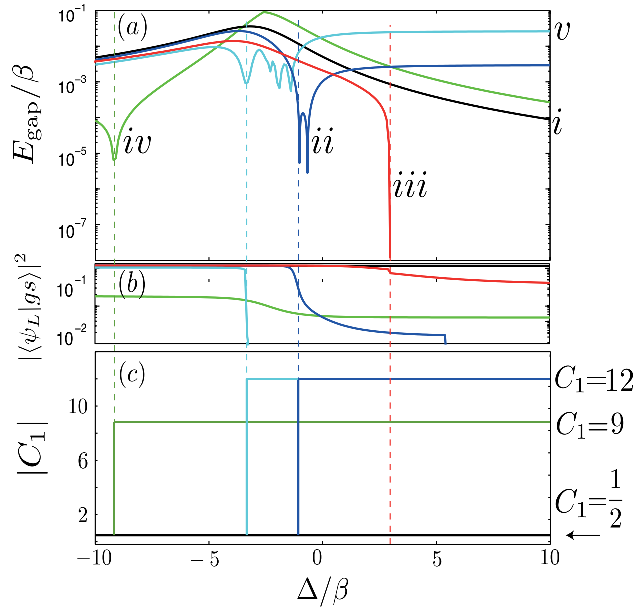

FIG. 3 (color online). (a) Energy gaps, (b) Laughlin wave function overlap, and (c) Chern numbers in the JCH FQHE as a function of the detuning Δ. For $\Delta \ll 0$, the effective on-site energy is very high. In the opposite case, where $\Delta \gg 0$, the effective on-site energy is much lower than the energy from the pressure and the gap is due to multiple site occupancy. Dashed lines indicate the transition from a fractional $1/2$ state to a noninteracting particle state as determined by the Chern number. Colors correspond to configurations in Table I: *i*, black; *ii*, dark blue; *iii*, red; *iv*, green; *v*, light blue.

of the Hall conductance in the edged geometry. This measure provides a means of classifying the ground state when the Laughlin ansatz is no longer a good representation. This circumstance occurs when lattice effects become significant, such as with large α, when the single-particle states deviate significantly from the continuum LLLs. Hafezi *et al.* [38] have found Chern numbers for states in the BH model.

The degenerate ground states, $\Psi_0(\theta)$, define a principal fiber bundle over the T^2 manifold. The Chern number classifies the homotopy class of the fiber bundle, which is a topological invariant. That is, the Chern number is insensitive to small perturbations relative to the energy gap. Only if the gap closes can the transition to topologically different states occur. Explicit computation of Eq. (6) is computationally intensive. We instead use the method first proposed in [40] and used in [38], which allows for efficient computation of the Chern number in the presence of degeneracies. In this method, a phase is defined for the ground state at each $\theta_{x,y}$ with respect to two reference states. The Chern number is given as the signed sum of the vortices that occur at the zeros of the overlap with one of the reference states.

Figures 3(a) and 3(c) plot the energy gap and Chern number, respectively, as a function of Δ. Both indicate that, for some lattice configurations, a transition occurs from the FQHE state to some uncorrelated states. In the JCH model (and BH), the discrete lattice gives rise to pressure in the system. Competition between this pressure and the on-site repulsion leads to a topological phase transition. In the limit of weak interactions, the pressure dominates, and the ground state is defined by single-particle behavior. Between these two limits, the energy gap closes at a single point in momentum space, marking the transition to a fractional state. Shown in Table I for a range of lattice configurations (*i*–*vi*) is the Laughlin wave-function overlap and the location of the value of Δ at which the transition occurs. We find that in the case of configurations *i* and *vi*, no such transition occurs due to an exact degeneracy in the single-particle energy spectrum. Before the transition, the ground state Chern number is $1/2$. When the gap closes, the Chern number changes discretely to the noninteracting state. The Chern number for the system is then the sum of Chern numbers for single particles, given by solutions to the Diophantine equation $C_1 = sq/p - 1/q$, $(s, C_1) \in \mathbb{N}$ [41]. We find this to be the case for configurations *ii*, *vii* and *v*. For *iii*, C_1 is undefined due to the presence of level crossings, as we have also observed in the case of the BH model. The question of whether these transitions persist in the thermodynamic limit is still an open question [38].

The proposed system can potentially be implemented in any cavity QED framework. However, circuit QED systems are the most promising, as they exhibit the largest atom-photon interactions relative to cavity Q. With coherence times for qubits approaching 10 μs [42] and coupling strengths $\approx 10^2$ MHz [43], FQHE states on small lattices, on the order of 15 sites, could be produced.

We have shown that many of the phenomena associated with the FQHE can be realistically emulated in cavity QED systems. Cavity lattices allow direct inspection of quantum states, which offers an unprecedented window into the physics of the QHE and topological phases. The cavity QED framework also allows for very broad control over the system's parameters and is readily extensible to more complicated configurations. For example, photons can be given an effective three-body contact interaction [44]. Three-body interactions in the electronic QHE system can lead to Pfaffian states [45]. These states have non-Abelian statistics and are a basis for the description of the $\nu = 5/2$ quantum Hall plateau. An implementation of the system considered in this Letter is an exciting prospect for the near future and will provide crucial insight into the physics of the quantum Hall effect.

A. D. G. acknowledges the Australian Research Council for financial support (Project No. DP0880466).

[1] I. Buluta and F. Nori, Science **326**, 108 (2009).
[2] M. Lewenstein, A. Sanpera, V. Ahufinger, B. Damski, A. Sen(de), and U. Sen, Adv. Phys. **56**, 243 (2007).

[3] A. van Oudenaarden and J. E. Mooij, Phys. Rev. Lett. **76**, 4947 (1996).
[4] S. Mostame and R. Schützhold, Phys. Rev. Lett. **101**, 220501 (2008).
[5] M. J. Hartmann, F. G. S. L. Brandao, and M. B. Plenio, Nature Phys. **2**, 849 (2006).
[6] A. D. Greentree, C. Tahan, J. H. Cole, and L. C. L. Hollenberg, Nature Phys. **2**, 856 (2006).
[7] D. Angelakis, M. Santos, and S. Bose, Phys. Rev. A **76**, 031805 (2007).
[8] N. Na, S. Utsunomiya, L. Tian, and Y. Yamamoto, Phys. Rev. A **77**, 031803 (2008).
[9] S.-C. Lei and R.-K. Lee, Phys. Rev. A **77**, 033827(2008).
[10] K. M. Birnbaum, A. Boca, R. Miller, A. D. Boozer, T. E. Northup, and H. J. Kimble, Nature (London) **436**, 87 (2005).
[11] A. A. Houck *et al.*, Nature (London) **449**, 328 (2007).
[12] M. Notomi, E. Kuramochi, and T. Tanabe, Nature Photon. **2**, 741 (2008).
[13] G. Lepert, M. Trupke, M. J. Hartman, M. B. Plenio, and E. A. Hinds, New J. Phys. **13**, 113002 (2011).
[14] K. v. Klitzing, G. Dorda, and M. Pepper, Phys. Rev. Lett. **45**, 494 (1980).
[15] D. C. Tsui, H. L. Stormer, and A. C. Gossard, Phys. Rev. Lett. **48**, 1559 (1982).
[16] K. I. Bolotin, F. Ghahari, M. D. Shulman, H. L. Stormer, and P. Kim, Nature (London) **462**, 196 (2009).
[17] M. Storni, R. H. Morf, and S. Das Sarma, Phys. Rev. Lett. **104**, 076803 (2010).
[18] R. B. Laughlin, Phys. Rev. Lett. **50**, 1395 (1983).
[19] D. Jaksch and P. Zoller, New J. Phys. **5**, 56 (2003).
[20] A. Sørensen, E. Demler, and M. Lukin, Phys. Rev. Lett. **94**, 076803 (2005).
[21] A. R. Kolovsky, Europhys. Lett. **93**, 20003 (2011).
[22] A. Fetter, J. Low Temp. Phys. **161**, 445 (2010).
[23] J. Quach, M. I. Makin, C. H. Su, A. D. Greentree, and L. C. L. Hollenberg, Phys. Rev. A **80**, 063838 (2009).
[24] S.-C. Lei, T.-K. Ng, and R.-K. Lee, Opt. Express **18**, 14586 (2010).
[25] J. Q. Quach, C. H. Su, A. M. Martin, A. D. Greentree, and L. C. L. Hollenberg, Opt. Express **19**, 11018 (2011).
[26] D. Rossini and R. Fazio, Phys. Rev. Lett. **99**, 186401 (2007).
[27] M. Hohenadler, M. Aichhorn, S. Schmidt, and L. Pollet, Phys. Rev. A **84**, 041608 (2011).
[28] M. I. Makin, J. H. Cole, C. D. Hill, A. D. Greentree, and L. C. L. Hollenberg, Phys. Rev. A **80**, 043842 (2009).
[29] J. Cho, D. Angelakis, and S. Bose, Phys. Rev. Lett. **101**, 246809 (2008).
[30] R. Yu, W. Zhang, H.-J. Zhang, S.-C. Zhang, X. Dai, and Z. Fang, Science **329**, 61 (2010).
[31] J. Koch, A. A. Houck, K. Le Hur, and S. M. Girvin, Phys. Rev. A **82**, 043811 (2010).
[32] A. Nunnenkamp, J. Koch, and S. M. Girvin, New J. Phys. **13**, 095008 (2011).
[33] M. Sandberg, F. Persson, I. C. Hoi, C. M. Wilson, and P. Delsing, Phys. Scr. **T137**, 014018 (2009).
[34] J. R. Johansson, G. Johansson, C. M. Wilson, and F. Nori, Phys. Rev. Lett. **103**, 147003 (2009).
[35] D. Hofstadter, Phys. Rev. B **14**, 2239 (1976).
[36] M. I. Makin, J. H. Cole, C. Tahan, L. C. L. Hollenberg, and A. D. Greentree, Phys. Rev. A **77**, 053819 (2008).
[37] N. Read and E. Rezayi, Phys. Rev. B **54**, 16864 (1996).
[38] M. Hafezi, A. S. Sørensen, E. Demler, and M. D. Lukin, Phys. Rev. A **76**, 023613 (2007).
[39] R. Tao and F. D. M. Haldane, Phys. Rev. B **33**, 3844 (1986).
[40] Y. Hatsugai, J. Phys. Soc. Jpn. **73**, 2604 (2004).
[41] N. Goldman, J. Phys. B **42**, 055302 (2009).
[42] H. Paik *et al.*, Phys. Rev. Lett. **107**, 240501 (2011).
[43] L. S. Bishop, J. M. Chow, Jens Koch, A. A. Houck, M. H. Devoret, E. Thuneberg, S. M. Girvin, and R. J. Schoelkopf, Nature Phys. **5**, 105 (2008).
[44] A. B. Matsko, I. Novikova, M. S. Zubairy, and G. R. Welch, Phys. Rev. A **67**, 043805 (2003).
[45] M. Greiter, X. G. Wen, and F. Wilczek, Nucl. Phys. **B374**, 567 (1992).